A Consideration on High Accuracy Estimation of Successive Moving Baseline for a Slow Speed Robot Based on GNSS Positioning

Hiroki Hayashi
Department of Electrical and Electronic Engineering
Ritsumeikan University
Kusatsu, Japan
re0143ki@ed.ritsumei.ac.jp

Fumihito Umemura
Department of Electrical and Electronic Engineering
Ritsumeikan University
Kusatsu, Japan
re0149pf@ed.ritsumei.ac.jp

Yoshiharu Koya
Department of Electronic Engineering
Kobe City College of Technology
Kobe, Japan
koya@kobe-kosen.ac.jp

Yukihiro Kubo
Department of Electrical and Electronic Engineering
Ritsumeikan University
Kusatsu, Japan
ykubo@se.ritsumei.ac.jp

***Abstract*—GNSS (Global Navigation Satellite System) is currently used in a variety of applications, and its positioning accuracy requirements become more and more demanding. We focus on an automatic strawberry pollination robot (under development in Kobe City College of Technology) and study a method of successive moving baseline vector estimation. In this paper, we propose a method to estimate accurate successive moving baseline vectors based on the difference of the single GNSS receiver observables obtained at two successive observation time (epoch). Furthermore, we also propose a method to estimate the bias error included in the solution of the moving baseline vector. Throughout the experiment, the proposed method and the relative positioning method are compared, and the results show that the proposed method can provide the baseline vector with the accuracy of 1.06 cm.**

***Index Terms*—GNSS, Point positioning, Relative positioning, Kalman filter**

I. Introduction

GNSS is currently used in a variety of applications [1], and its positioning accuracy requirements become more and more demanding. In this paper, we focus on an automatic strawberry pollination robot that repeatedly moves and stops at low speed about less than 1 meter per 1 minute.

A. Strawberry Pollination Robot

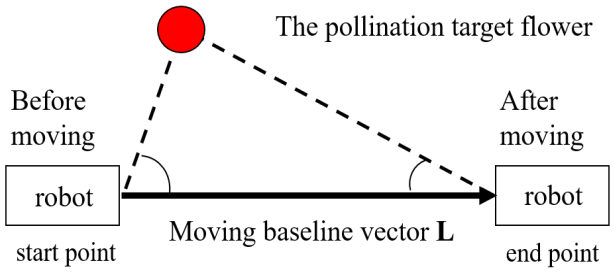

Fig. 1. Strawberry Pollination Robot

Fig. 1 shows the image of strawberry pollination robot. The strawberry pollination robot searches for the target strawberry's flower using single camera and pollinates automatically by the robot arm in strawberry field [2]. To pollinate precisely, the angle and three dimensional position from robot to the target flower are required. The robot equipped single camera moves and takes two images of the flower at the start and end point. The relative angle and the three dimensional position of the flower from the robot can be obtained by applying the moving stereo image processing technique, e.g. [3] to the images. In order to implement the stereo image processing precisely, the moving baseline vector need to be precisely estimated. In this paper, we propose a method to estimate the moving baseline vector by using the single GNSS receiver [4], [5].

B. Concept of Proposed Method

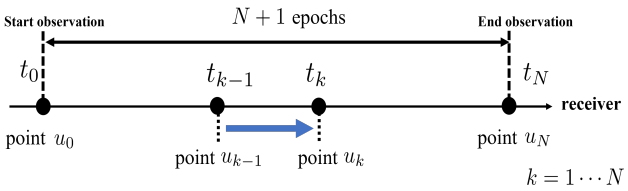

Fig. 2. Proposed Method

In this paper, we propose a method to estimate accurate successive moving baseline vectors based on the difference of the GNSS receiver observables obtained at two successive observation time (epoch). Fig. 2 shows the relation between the observation epoch and the position of the robot. The position at epoch k (time t_k) is denoted by u_k, and the robot moves from u_0 to u_N, where $t_k \equiv t_0 + k\Delta T$ and ΔT is the sampling interval.

The concept of the proposed method is to estimate the moving baseline vector between two successive epochs $u_k - u_{k-1}$ based on the difference of observables at k and $k-1$

that are obtained by one receiver. By summing the estimated moving baseline vectors, we can also obtain the position of the robot relative to the start point u_0. In this paper, we consider the case that the baseline length from u_0 to u_N is about 1 meter for 1 minute, and the sampling time interval is 1 second, i.e. $\Delta T = 1$.

The idea of the proposed method is based on the so-called moving base method proposed in [6], [7]. In [6], [7], the relative position between two moving receivers are obtained with millimeter to centimeter level accuracy. The principle of the moving base is similar to the relative positioning method [8] which can provide the highest accuracy in GNSS positioning methods. In this paper, we modify the moving base method and apply it to the one receiver case. If the sampling time interval is sufficiently short, e.g. less than 5 [s], almost same accuracy of the moving base method can be expected. Although highly accurate estimates of the moving baseline vector are expected by the relative positioning, it is widely known that they have small (millimeter level for short baseline) errors. The small errors are mainly caused by the surrounding environments, and can be regarded as bias errors within several minutes. In this paper, therefore, we also propose a method to estimate the bias error utilizing the estimation results during the robot stops. And we correct the estimated moving baseline vector by the estimated bias when the robot in moving.

II. Measurement Models and Moving Baseline Estimation

Hereafter, the model of observables is shown for only GPS (Global Positioning System) of the U.S. [9], [10], and it can be easily extended to other satellite systems. Let $\rho_i^p(k)$ denote the code pseudorange observation of satellite p at epoch k. The subscript i is the index of the type of code pseudorange, such that $i = 1$ means C/A code and $i = 2$ means P(Y) code. Similarly, let $\Phi_j^p(k)$ denote the carrier phase observation. The subscript j is the index of the frequency band, such that $j = 1$ means L1 band and $j = 2$ means L2 band [8], [11]. They are typically expressed as follows:

$$\begin{aligned}\rho_1^p(k)=&r^p(k) + c\{\delta t(k) - \delta t^p(k)\} + \delta I^p(k)\\ &+\delta T^p(k) + e_1^p(k),\end{aligned} \tag{1}$$

$$\begin{aligned}\rho_2^p(k)=&r^p(k) + c\{\delta t(k) - \delta t^p(k)\} + \frac{f_1^2}{f_2^2}\delta I^p(k)\\ &+\delta T^p(k) + e_2^p(k),\end{aligned} \tag{2}$$

$$\begin{aligned}\Phi_1^p(k)=&r^p(k) + c\{\delta t(k) - \delta t^p(k)\} - \delta I^p(k)\\ &+\delta T^p(k) + \lambda_1 N_1^p + \varepsilon_1^p(k),\end{aligned} \tag{3}$$

$$\begin{aligned}\Phi_2^p(k)=&r^p(k) + c\{\delta t(k) - \delta t^p(k)\} - \frac{f_1^2}{f_2^2}\delta I^p(k)\\ &+\delta T^p(k) + \lambda_2 N_2^p + \varepsilon_2^p(k),\end{aligned} \tag{4}$$

where c ($\approx 2.99792458\times10^8$ m/s) denotes the speed of light, $f_1(= 1575.42$ MHz) and λ_1 are central frequency and the wave length of the L1 carrier wave. Similarly, $f_2(= 1227.6$ MHz) and λ_2 are central frequency and the wave length of the L2 carrier wave, respectively. δI^p is the ionospheric delay, and δT^p is the tropospheric delay. N_j^p denotes carrier phase ambiguity between the satellite p and the receiver. e and ε are the observation noises. $\delta t(k)$ is the receiver clock error. $\delta t^p(k)$ is the satellite clock error.

$r^p(k)$ is the geometric distance between the receiver and the satellite p. Namely, $r^p(k) \equiv ||u_k - s^p(k)||$, where $u_k \equiv \left[x_k, y_k, z_k\right]^{\mathrm{T}}$ is the unknown user position, $s^p \equiv \left[x^p, y^p, z^p\right]^{\mathrm{T}}$ is the satellite position , and $||a||$ denotes the Euclidean norm of vector a.

Then, applying the 1st order Taylor series approximation around the a priori estimate $u_k = \hat{u}_k$, the linearized observation equations are obtained as follows:

$$\begin{aligned}\tilde{\rho}_1^p(k)=&\rho_1^p(k) - r_{\hat{u}_k}^p(k) + g_{\hat{u}_k}^p \hat{u}_k\\ =&g_{\hat{u}_k}^p(k)u_k + c\{\delta t(k) - \delta t^p(k)\} + \delta I^p(k)\\ &+\delta T^p(k) + e_1^p(k),\end{aligned} \tag{5}$$

$$\begin{aligned}\tilde{\rho}_2^p(k)=&\rho_2^p(k) - r_{\hat{u}_k}^p(k) + g_{\hat{u}_k}^p \hat{u}_k\\ =&g_{\hat{u}_k}^p(k)u_k + c\{\delta t(k) - \delta t^p(k)\} + \frac{f_1^2}{f_2^2}\delta I^p(k)\\ &+\delta T^p(k) + e_2^p(k),\end{aligned} \tag{6}$$

$$\begin{aligned}\tilde{\Phi}_1^p(k)=&\Phi_1^p(k) - r_{\hat{u}_k}^p(k) + g_{\hat{u}_k}^p \hat{u}_k\\ =&g_{\hat{u}_k}^p(k)u_k + c\{\delta t(k) - \delta t^p(k)\} - \delta I^p(k)\\ &+\delta T^p(k) + \lambda_1 N_1^p + \varepsilon_1^p(k),\end{aligned} \tag{7}$$

$$\begin{aligned}\tilde{\Phi}_2^p(k)=&\Phi_2^p(k) - r_{\hat{u}_k}^p(k) + g_{\hat{u}_k}^p \hat{u}_k\\ =&g_{\hat{u}_k}^p(k)u_k + c\{\delta t(k) - \delta t^p(k)\} - \frac{f_1^2}{f_2^2}\delta I^p(k)\\ &+\delta T^p(k) + \lambda_2 N_2^p + \varepsilon_2^p(k),\end{aligned} \tag{8}$$

where

$$r_{\hat{u}_k}^p(k) \equiv ||\hat{u}_k - s^p(k)||,$$

$$g_{\hat{u}_k}^p(k) \equiv \left[\frac{\partial r^p(k)}{\partial u_k}\right]_{u_k=\hat{u}_k}^{\mathrm{T}} = \frac{\{\hat{u}_k - s^p(k)\}^{\mathrm{T}}}{||\hat{u}_k - s^p(k)||}.$$

A. Satellite-Satellite Single Difference

If we also obtain the same types of observations for satellite q, we can eliminate errors caused by the receiver such as receiver clock error and receiver hardware bias, by differencing them. This is called the satellite-satellite single difference and can be expressed as follows:

$$\rho_i^{pq}(k) \equiv \rho_i^p(k) - \rho_i^q(k), \tag{9}$$

$$\Phi_j^{pq}(k) \equiv \Phi_j^p(k) - \Phi_j^q(k). \tag{10}$$

Based on the linearized equations (5)–(8), the single differences are expressed as follows:

$$\begin{aligned}\tilde{\rho}_1^{pq}(k)=&\tilde{\rho}_1^p(k) - \tilde{\rho}_1^q(k)\\ =&g_{\hat{u}_k}^p u_k - g_{\hat{u}_k}^q u_k + c(\delta t^q - \delta t^p) + \delta I^p - \delta I^q\\ &+\delta T^p - \delta T^q + e_1^p - e_1^q\\ =&g_{\hat{u}_k}^{pq} u_k + c\delta t^{qp} + \delta I^{pq} + \delta T^{pq} + e_1^{pq},\end{aligned} \tag{11}$$

$$\begin{aligned}\tilde{\rho}_2^{pq}(k)=&\tilde{\rho}_2^p(k) - \tilde{\rho}_2^q(k)\\ =&g_{\hat{u}_k}^p u_k - g_{\hat{u}_k}^q u_k + c(\delta t^q - \delta t^p) + \frac{f_1^2}{f_2^2}(\delta I^p - \delta I^q)\\ &+\delta T^p - \delta T^q + e_2^p - e_2^q\\ =&g_{\hat{u}_k}^{pq} u_k + c\delta t^{qp} + \frac{f_1^2}{f_2^2}\delta I^{pq} + \delta T^{pq} + e_2^{pq},\end{aligned} \tag{12}$$

$$\begin{aligned}\tilde{\Phi}_1^{pq}(k)=&\tilde{\Phi}_1^{p}(k)-\tilde{\Phi}_1^{q}(k)\\ =&g_{\hat{u}_k}^{p}u_k-g_{\hat{u}_k}^{q}u_k+c(\delta t^q-\delta t^p)-(\delta I^p-\delta I^q)\\ &+\delta T^p-\delta T^q+\lambda_1(N_1^p-N_1^q)+\varepsilon_1^p-\varepsilon_1^q\\ =&g_{\hat{u}_k}^{pq}u_k+c\delta t^{qp}-\delta I^{pq}+\delta T^{pq}\\ &+\lambda_1 N_1^{pq}+\varepsilon_1^{pq}, \end{aligned}\tag{13}$$

$$\begin{aligned}\tilde{\Phi}_2^{pq}(k)=&\tilde{\Phi}_2^{p}(k)-\tilde{\Phi}_2^{q}(k)\\ =&g_{\hat{u}_k}^{p}u_k-g_{\hat{u}_k}^{q}u_k+c(\delta t^q-\delta t^p)-\frac{f_1^2}{f_2^2}(\delta I^p-\delta I^q)\\ &+\delta T^p-\delta T^q+\lambda_2(N_2^p-N_2^q)+\varepsilon_2^p-\varepsilon_2^q\\ =&g_{\hat{u}_k}^{pq}u_k+c\delta t^{qp}-\frac{f_1^2}{f_2^2}\delta I^{pq}+\delta T^{pq}\\ &+\lambda_2 N_2^{pq}+\varepsilon_2^{pq}, \end{aligned}\tag{14}$$

where

$$\begin{aligned} g_{\hat{u}_k}^{pq}\equiv&g_{\hat{u}_k}^{p}-g_{\hat{u}_k}^{q},\\ \delta t^{qp}\equiv&\delta t^{q}-\delta t^{p},\\ \delta I^{pq}\equiv&\delta I^{p}-\delta I^{q},\\ \delta T^{pq}\equiv&\delta T^{p}-\delta T^{q},\\ N_j^{pq}\equiv&N_j^{p}-N_j^{q},\\ e_i^{pq}\equiv&e_i^{p}-e_i^{q},\\ \varepsilon_j^{pq}\equiv&\varepsilon_j^{p}-\varepsilon_j^{q}. \end{aligned}$$

B. Single Difference Between Two Epochs

Similarly, the satellite-satellite single difference can be obtained for epoch $k-1$. Furthermore, by differencing these successive single differences, errors due to satellite side such as satellite clock error, tropospheric and ionospheric effects, and carrier phase ambiguity can be eliminated because they are rigorously constant or considered to be constant within a short time span. Finally, code pseudorange and carrier phase observations in the proposed method are formulated as follows:

$$\begin{aligned}\rho_i^{pq}(k,k-1)\equiv&\rho_i^{pq}(k)-\rho_i^{pq}(k-1)\\ =&\rho_i^{p}(k)-\rho_i^{q}(k)\\ &-\rho_i^{p}(k-1)+\rho_i^{q}(k-1), \end{aligned}\tag{15}$$

$$\begin{aligned}\Phi_j^{pq}(k,k-1)\equiv&\Phi_j^{pq}(k)-\Phi_j^{pq}(k-1)\\ =&\Phi_j^{p}(k)-\Phi_j^{q}(k)\\ &-\Phi_j^{p}(k-1)+\Phi_j^{q}(k-1). \end{aligned}\tag{16}$$

Based on the linearized expression (11)–(14), and substituting the a priori estimate $\hat{u}_k$ by $\hat{u}_{k-1}$ for linearization such that $g_{\hat{u}_{k-1}}^{p}(k)\equiv\left[\frac{\partial r^p(k)}{\partial u_k}\right]^{\mathrm{T}}_{u_k=\hat{u}_{k-1}}$, we obtain

$$\begin{aligned}\tilde{\rho}_1^{pq}(k,k-1)=&g_{\hat{u}_{k-1}}^{pq}(u_k-\hat{u}_{k-1})+c\delta t^{qp}(k,k-1)\\ &+\delta I^{pq}(k,k-1)+\delta T^{pq}(k,k-1)\\ &+e_1^{pq}(k,k-1), \end{aligned}\tag{17}$$

$$\begin{aligned}\tilde{\rho}_2^{pq}(k,k-1)=&g_{\hat{u}_{k-1}}^{pq}(u_k-\hat{u}_{k-1})+c\delta t^{qp}(k,k-1)\\ &+\frac{f_1^2}{f_2^2}\delta I^{pq}(k,k-1)+\delta T^{pq}(k,k-1)\\ &+e_2^{pq}(k,k-1), \end{aligned}\tag{18}$$

$$\begin{aligned}\tilde{\Phi}_1^{pq}(k,k-1)=&g_{\hat{u}_{k-1}}^{pq}(u_k-\hat{u}_{k-1})+c\delta t^{qp}(k,k-1)\\ &-\delta I^{pq}(k,k-1)+\delta T^{pq}(k,k-1)\\ &+\lambda_1 N_1^{pq}(k,k-1)\\ &+\varepsilon_1^{pq}(k,k-1), \end{aligned}\tag{19}$$

$$\begin{aligned}\tilde{\Phi}_2^{pq}(k,k-1)=&g_{\hat{u}_{k-1}}^{pq}(u_k-\hat{u}_{k-1})+c\delta t^{qp}(k,k-1)\\ &-\frac{f_1^2}{f_2^2}\delta I^{pq}(k,k-1)+\delta T^{pq}(k,k-1)\\ &+\lambda_2 N_2^{pq}(k,k-1)\\ &+\varepsilon_2^{pq}(k,k-1). \end{aligned}\tag{20}$$

In (17)–(20), $g_{\hat{u}_{k-1}}^{pq}$ is a known 1×3 vector. Also, the difference of satellite clock error

$$\delta t^{qp}(k,k-1)\equiv\delta t^{qp}(k)-\delta t^{qp}(k-1),$$

and the ionospheric and tropospheric delays

$$\begin{aligned}\delta I^{pq}(k,k-1)\equiv&\delta I^{pq}(k)-\delta I^{pq}(k-1),\\ \delta T^{pq}(k,k-1)\equiv&\delta T^{pq}(k)-\delta T^{pq}(k-1)\end{aligned}$$

are negligible for short baseline and short time span. The carrier phase ambiguity

$$N_j^{pq}(k,k-1)\equiv N_j^{pq}(k)-N_j^{pq}(k-1)$$

is rigorously zero as long as the receiver continuously tracks the satellite signal.

Therefore, finally, we obtain the observation equations for moving baseline estimation in a very simple expression as follows:

$$\tilde{\rho}_i^{pq}(k,k-1)=g_{\hat{u}_{k-1}}^{pq}(u_k-\hat{u}_{k-1})+e_i^{pq}(k,k-1),\tag{21}$$

$$\tilde{\Phi}_j^{pq}(k,k-1)=g_{\hat{u}_{k-1}}^{pq}(u_k-\hat{u}_{k-1})+\varepsilon_j^{pq}(k,k-1),\tag{22}$$

where

$$\begin{aligned}e_i^{pq}(k,k-1)=&e_i^{pq}(k)-e_i^{pq}(k-1),\\ \varepsilon_j^{pq}(k,k-1)=&\varepsilon_j^{pq}(k)-\varepsilon_j^{pq}(k-1).\end{aligned}$$

C. Moving Baseline Estimation

Since the robot moves at low speed, assuming its small velocity can be expressed by small Gaussian white noises, the state equation is expressed by equation (23).

$$x(k+1)=x(k)+w(k),\tag{23}$$

where

$$x(k)\equiv u_k-\hat{u}_{k-1}.$$

For multiple satellites ($p=1, q=2,\cdots,n_s$), the observables in equations (21) and (22) are expressed as vectors y_i and y_j, e.g. $y_i\equiv[\rho_i^{12},\rho_i^{13},\cdots,\rho_i^{1n_s}]^{\mathrm{T}}$. Similarly, observation noises $e_i^{pq}(k,k-1)$ and $\varepsilon_j^{pq}(k,k-1)$ in (21) and (22) are expressed as vectors e_i and ε_j, e.g. $e_i\equiv[e_i^{12},e_i^{13},\cdots,e_i^{1n_s}]^{\mathrm{T}}$. The whole observation equation can be expressed as equation (24).

$$y(k)=H(k)x(k)+v(k),\tag{24}$$

where

$$y(k)\equiv\begin{bmatrix}y_i\\ y_j\end{bmatrix},\ H(k)\equiv\begin{bmatrix}G^{pq}\\ G^{pq}\end{bmatrix},\ v(k)\equiv\begin{bmatrix}e_i\\ \varepsilon_j\end{bmatrix},$$

$$G^{pq} \equiv \left[\; {g^{12}_{\hat{u}_{k-1}}}^{\mathrm{T}}, \quad {g^{13}_{\hat{u}_{k-1}}}^{\mathrm{T}}, \quad \cdots, \quad {g^{1n_s}_{\hat{u}_{k-1}}}^{\mathrm{T}} \; \right]^{\mathrm{T}}.$$

The Kalman filter is applied to equations (23) and (24) to estimate the robot's moving baseline vector $u_k - \hat{u}_{k-1}$ [12]–[14]. Finally, we obtain the position $u_k = \hat{u}_k$ at epoch k by adding the moving baseline vector $u_k - \hat{u}_{k-1}$ to the position $u_{k-1} = \hat{u}_{k-1}$ at epoch $k-1$.

The filtered estimate of the above Kalman filter, which is denoted by $\hat{x}(k|k)$, is the estimate of the moving baseline vector between epochs k and $k-1$. Therefore, let $\hat{L}_N$ the moving baseline L in Fig. 1, and it can be obtained by summing $\hat{x}(k|k)$ for $k = 1, \cdots N$ as follows:

$$\hat{L}_N = \sum_{k=1}^{N} \hat{x}(k|k). \tag{25}$$

Also, the position $u_N = \hat{u}_N$ relative to the starting position u_0 can be obtained as follows:.

$$\hat{u}_N = \hat{L}_N + u_0. \tag{26}$$

III. The Bias Error Estimation

It is well known, in the GNSS community, that the baseline vector can be obtained with excellent accuracy by so-called RTK (Real Time Kinematic) method [15]. For example, according to the specification of the typical GNSS receiver [16], the horizontal accuracy (RMS value)
$0.6 + (0.5 \times 10^{-6} \times$ baseline length) centimeters is achieved.

The method proposed in this paper is not the RTK method. On the other, for the situation of the short baseline and short time span, that is the assumptions in this paper, we can consider that the similar principle which provides highly accurate solution of the RTK method is also employed in the proposed method. Therefore, it is expected that the estimated moving baseline vector between successive epochs, i.e. $\hat{x}(k|k)$, has almost the same accuracy as the RTK method.

However, it is also well known that the small error in RTK solution mainly depends on surrounding environment such as buildings, as well as satellite's constellation. And the small error varies slowly as it can be recognized as the constant bias in the period of several minutes. In the proposed method, the estimated baseline vector between successive epochs are summed as shown in (25). Although the error is small (millimeter level) individually, the sum will be large as a few centimeters to several tens of centimeters.

To overcome this problem, we also propose a simple but effective method to mitigate the influence of the small error in $\hat{x}(k|k)$. In order to describe the algorithm, now we assume the robot keeps stopping from time t_0 to t_M, and $M+1$ epochs GNSS observation data are collected at position $u_0 = u_1 = \cdots = u_M$, see Fig. 2 by substituting N by M. Then, by applying the method in Section II, we obtain the moving baseline vector as (25). Here, it is denoted by $\hat{L}_{s,M}$, where the subscripts "$s,\ M$" mean the estimate based on "s"topping, "M" epochs data. So that

$$\begin{aligned} \hat{L}_{s,M} &= \sum_{k=1}^{M} \hat{x}(k|k) \\ &= \sum_{k=1}^{M} (x(k) + b). \end{aligned} \tag{27}$$

The vector $x(k)$ is theoretically a zero vector because the robot keeps stopping in this period. By assuming the small error in $\hat{x}(k|k)$, which is denoted by b, is the constant for $M+1$ epochs, we can obtain the estimate of b as

$$\hat{b} = \frac{\hat{L}_{s,M}}{M}. \tag{28}$$

Therefore, we estimate $\hat{b}$ prior to the robot motion, the bias error mitigation can be implemented by

$$\hat{L}_{b,N} = \sum_{k=1}^{N} (\hat{x}(k|k) - \hat{b}). \tag{29}$$

Similarly, the position $u_N = \hat{u}_N$ of (26) is corrected as follows:

$$\hat{u}_{b,N} = \hat{L}_{b,N} + u_0. \tag{30}$$

IV. Experimental Results

We have carried out experiments under the open sky environment and applied proposed method to real receiver data. Table I shows experimental conditions. Through all the observation epochs, the satellite constellation was the same. The total number of satellites was 5 ($n_s = 5$), and we selected the satellite with highest elevation angle as the reference satellite ($p = 1$) for single differencing operation described in II-A.

TABLE I
Experimental Conditions

Date	April 20, 2022
Location	Biwako-Kusatsu Campas, Ritsumeikan University
Observation Data(GPST)	09:35'00–09:50'00
Antenna	ANN-MB-00-00(u-blox)
Receiver	AsteRx-m2 UAS(Septentrio) FLEX6(NovAtel)
Sampling Interval	1 [s]
Elevation Mask	30 [deg.]
Measurement Data	C/A P(Y) code pseudorange L1 L2 carrier-phase
Used Satellite	GPS

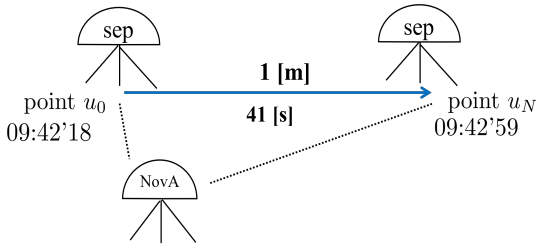

Fig. 3. Experiment Situation

The robot stopped at u_0 for 2 minutes, then it started moving at t_0 =09:42'18, and after 41 seconds ($N = 41$), it reached u_N at t_N =09:42'59 (see Fig. 3). The distance moved was 1 m, which was measured by using a tape measure.

The GNSS receiver AsteRx-m2 UAS of Septentrio was equipped on the robot. Furthermore, to evaluate the accuracy of the proposed method, another receiver, that is FLEX6 of NovAtel fixed about 2 m aware from the robot collected

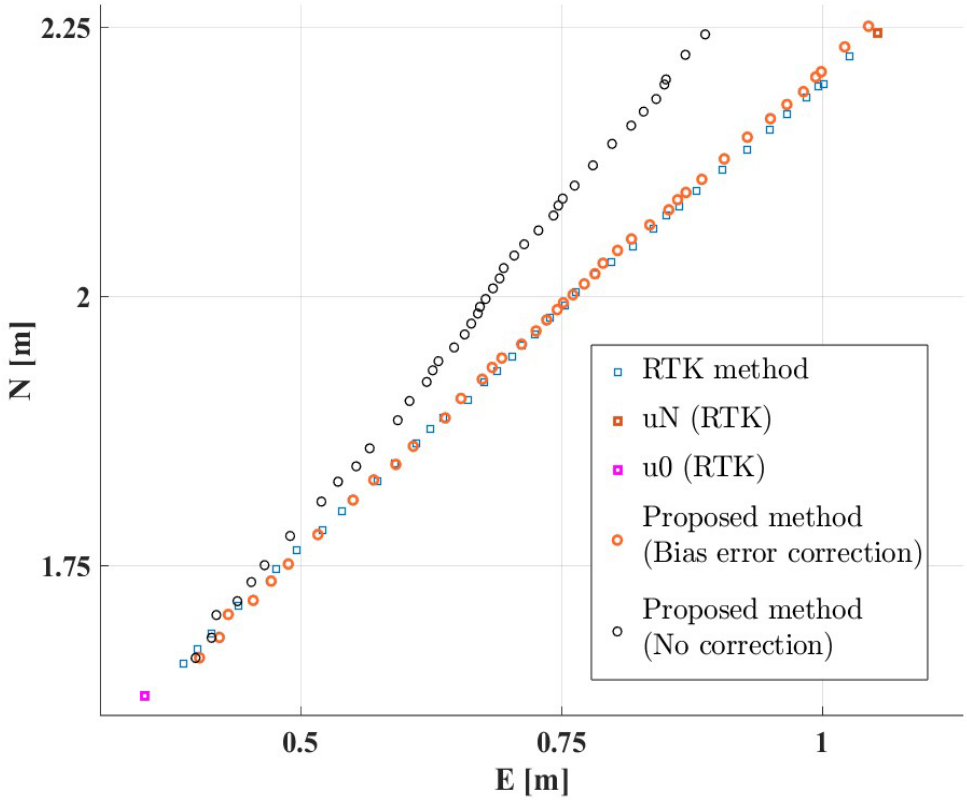

Fig. 4. The Experimental Results of the Horizontal Coordinates

GNSS data simultaneously. Here, the performance of the proposed method is evaluated by regarding the traditional relative positioning (RTK) result between AsteRx-m2 and FLEX6 as the reference trajectory.

Based on the 2 minutes GNSS data, that were collected prior to the movement, the estimated small error (bias error in $\hat{x}(k|k)$), i.e. $\hat{b}$ of (28) was

$$\hat{b} = [5.542, 0.004534, -3.058]^{\mathrm{T}} \times 10^{-3} \text{ m}.$$

Fig. 4 shows the estimates of the horizontal coordinates of the robot. The pink and red square symbols show the point u_0 and u_N obtained by the RTK method, respectively. Also, the blue square symbols show the trajectory by the RTK method. So, the square symbols are recognized as the refence (true) for evaluating the proposed method. The horizontal axis shows the coordinates of the east direction, and the vertical one shows the north direction, where the origin shows the position of FLEX6 receiver. In Fig. 4, the estimated coordinates of the robot by the proposed method without the bias correction, that is $\hat{L}_N$ for $N = 1, \cdots 41$ are shown by the black circle symbols. Also, the estimates with bias correction, that is $\hat{L}_{b,N}$ for $N = 1, \cdots 41$ are shown by the orange circle symbols.

Now, focusing on the point u_N where is the point of the end of movement, the error of estimated position was 16 cm in $\hat{L}_{41}$ (without bias correction), and 1.06 cm in $\hat{L}_{b,41}$ (with bias correction).

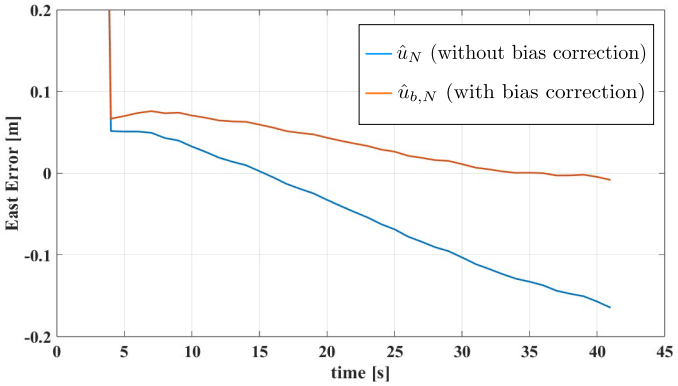

Fig. 5. East Position Errors

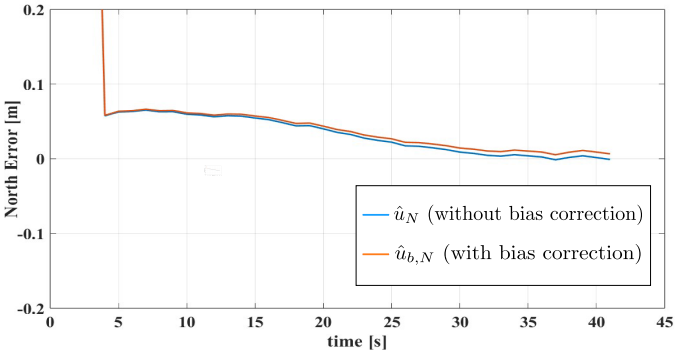

Fig. 6. North Position Errors

We also focus on the circle symbols by the proposed methods and square symbols by the RTK method. Fig. 5 shows the relation between the observation time and the east direction error of estimated position. Similarly, Fig. 6 shows the relation between the observation time and the north direction error of estimated position. The east error of the estimated position was 16.5 cm in $\hat{L}_{41}$ (final value of the blue line) and 0.82 cm in $\hat{L}_{b,41}$ (final value of the orange line). The north error of estimated position was 0.082 cm in $\hat{L}_{41}$ and 0.67 cm in $\hat{L}_{b,41}$, both within 1 cm accuracy.

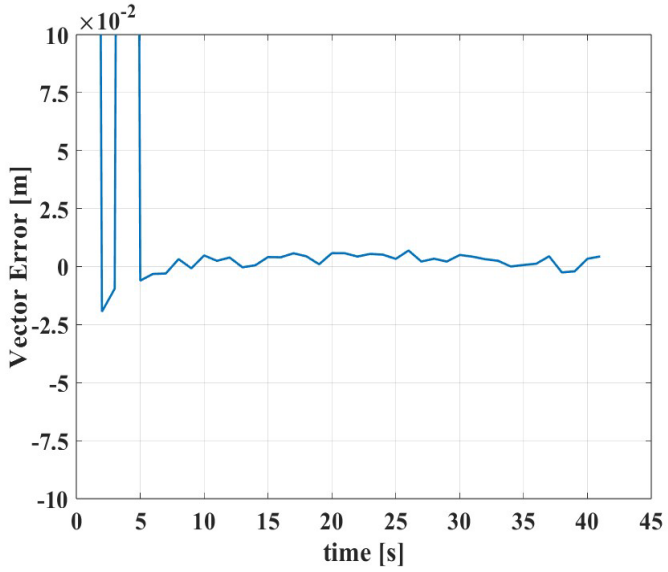

Fig. 7. The Accuracy of the Moving Baseline Vector

Furthermore, the accuracy of the moving baseline vector $\hat{x}(k|k)$ is shown in Fig. 7. The horizontal axis shows the observation time, and the vertical one shows the error of the moving baseline vector estimated by the proposed method and the RTK method. The error was finally 0.44 cm.

It can be seen from these results that the idea of bias correction of Section III is very effective and the moving baseline L is estimated precisely by the proposed method with the bias correction.

V. Conclusions

In this paper, we proposed the new method to estimate the short moving baseline vector of slowly moving robot by using the single GNSS receiver. The algorithm is based on the difference of the successive two epochs GNSS observables.

Also, we proposed the simple but effective algorithm to mitigate the influence of the small bias like estimation error in the baseline vector between two successive epochs. From the results of experiments, we can see that the proposed algorithm achieves less than about 1 centimeter accuracy for 1 meter movement in several tens of seconds, and it is almost the same performance of the traditional high accuracy RTK method.

In the future study, we will evaluate the algorithm for various kind of situations such as periods for estimating the bias like error b, satellite constellation, as well as for the real moving robot.

The proposed method assume that the robot moves at low speed about less than 1 meter per 1 minute. Therefore, we will also consider the algorithm in terms of speed as well, such as by adding the Doppler observable to the observation equation (24) and improving the state equation (23), to see how the increase of the robot's speed affects the accuracy of the proposed method.

References

[1] The Geodetic Society of Japan (Eds.), Global Positioning System - Precise Positioning System by Artificial Satellite, New Edition, Japan Association of Surveyors, 1989 (in Japanese).

[2] K. Sumiyama, Y. Koya, and Y. Kubo, "The automatic pollination robot targeted strawberry flower," *Kansai-section Joint Convention of Institutes of Electrical Engineering*, pp.42-43, Shiga, November, 2020 (in Japanese).

[3] H. Tamura, The Computer Image Processing, Ohmsha, Tokyo, 2002 (in Japanese).

[4] H. Hayashi, N. Sasamoto, Y. Koya, and Y. Kubo, "A Method of Successive Moving Baseline Estimation of a Slow Speed Robot Based on GNSS positioning," Proceedings of the 4th Society for the Advancement of Positioning Technologies, pp.8-16, Osaka, September, 2022.

[5] H. Hayashi, N. Sasamoto, Y. Koya, and Y. Kubo, "A Method of Successive Moving Baseline Estimation of a Slow Speed Robot Based on GNSS positioning," Proceedings of the 54th ISCIE International Symposium on Stochastic Systems Theory and Its Applications, pp.8-16, Nara, October, 2022.

[6] Y. Dong, L. Zhang, D. Wang, Q. Li, J. Wu, and M. Wu, "Low-latency, high-rate, high-precision relative positioning with moving base in real time," *GPS Solutions*, Vol. 24, issue 2, Article 56, pp.1-13, April, 2020.

[7] Z. Liang, L. Hanfeng, W. Dingjie, H. Yanqing, and W. Jie, "Asynchronous RTK precise DGNSS positioning method for deriving a low-latency high-rate output," *Journal of Geodesy*, Vol. 89, issue 7, pp.641-653, July, 2015.

[8] S. Sugimoto and R. Shibasaki (Eds.), *GPS Handbook*, Asakura, Tokyo, 2010 (in Japanese).

[9] E. D. Kaplan (Eds.), *Understanding GPS: Principles and Applications*, Artech House, Boston, 1996.

[10] B. W. Parkinson and J. J. Spilker Jr. (Eds.), *Global Positioning System: Theory and Applications, Vol. I, II*, AIAA, Washington, DC, 1997.

[11] P. Misra and P. Enge, *Global Positioning System - Signals, Measurements, and Performance, Second Edition*, Ganga-Jamuna Press, Massachusetts, 2006.

[12] T. Katayama, *Applied Kalman filter, New Edition*, Asakura, Tokyo, 2000 (in Japanese).

[13] S. Adachi and I. Maruda, *Fundamentals of Kalman filter*, Tokyo Denki University Press, Tokyo, 2012 (in Japanese).

[14] A. Gelb, *Applied Optimal Estimation*, MIT Press, Massachusetts, 1974.

[15] B. Hofmann-Wellenhof, H. Lichtenegger, and J. Collins, *Global Positioning System Theory and Practice, Third, revised edition*, Springer-Verlag, New York, 1994.

[16] The technical brochure of AsteRx-m2 UAS, Septentrio, https://pdf.directindustry.com/pdf/septentrio-183002.html, accessed on Sep. 15, 2022.